Bed rugosity determination for critical velocity profile in cohesionless sediment beds.

GARCÍA-ARAGÓN J.A , IZQUIERDO-AYALA K.,., SALINAS-TAPIA H. Y DÍAZ-DELGADO C.
Centro Interamericano de Recursos del Agua, Facultad de Ingeniería.
Universidad Autónoma del Estado de México.
Cerro de Coatepec, CU, Toluca, Edomex
MEXICO
Jagarcíaa@uaemex.mx http://www.uaemex.mx/cira

Abstract: Experimental results performed in a glass rectangular channel, with a loose bed in the central part where simulations of initiation of non-cohesive sediment motion for different grain sizes were developed, are presented in this paper. The optical technique of Particle Tracking Velocimetry (PTV) was used with the main goal of determination of critical velocity profiles for sediment initiation of motion. The parameter *ks* known as bed rugosity is difficult to obtain. For conditions near bed motion initiation velocity profiles were obtained and they allowed us to define a value of *ks* related to a representative grain size of the bed. It was shown that this bed rugosity is greater than the mean size of the bed, and the relative bed rugosity decreases when mean diameter increases. This finding should be taken into account when applying the different formulas for critical velocity in the scientific literature.

Key-Words: - non-cohesive sediments, motion initiation, bed rugosity, critical velocity profile PTV.

1. Introduction

In order to define the critical conditions for bed motion initiation in beds formed by cohesionless sediments a lot of work has been done [1]. The most known work is that of Shields [2] who, based on experimental data for bed motion initiation, related the bed shear stress to a dimensionless parameter. Yalin and Karahan [3] extended the findings to laminar flow. Later work for motion initiation has shown that the magnitude of critical shear stresses differs slightly from that of Shields but the shape of the curve is preserved ([4], [5], [1], [6], [7], [8], [9]). Research has been focused on the bed packing and sizes non-uniformities in order to obtain statistical parameters that relate in a better way the critical bed shear stress to a particle size parameter ([10], [11], [12]). River beds are constituted by a sediment mixture of different sizes and common engineering practice has been to extrapolate experimental data results with uniform size sediments to non-uniform sediment beds ([13], [14], [15]).

Bed rugosity is a parameter that represents the height of roughness of the bed. Nikuradse (cited by [1]) proposes for bed rugosity the mean diameter of the bed. In the case of non-uniform bed the largest diameters are intuitively more appropriate to represent bed rugosity. In the scientific literature it is common to represent bed rugosity as the mean diameter or another representative diameter multiplied by a factor larger than one. The problem is then to choose an appropriate representative diameter and an appropriate factor ([1], [16]).

The best representation of the interaction between the bed and the flow is the velocity profile. It has been shown that the best representation of the velocity profile is a logarithmic approximation, which includes a parameter named bed rugosity. Shear stress is implicitly represented in the velocity profile [16]. The critical velocity profile for bed motion initiation is defined as the velocity profile obtained when the critical shear stress is actuating. In this work this critical velocity profile was measured using the optical technique Particle Tracking Velocimetry (PTV) [17]. Five different combinations of shear stresses-critical velocity profile were obtained and bed rugosity was deduced for these five different sizes of sand at bed motion initiation.

Optical techniques like PTV are useful to measure turbulence and Reynolds stress distribution. This is a way to obtain the shear stress, also for difficult situations like in rivers where friction slope is not obtained straightforward. In this work shear velocity and shear

stress were obtained using the fluctuating velocities measured for each velocity profile ([18], [19]).

2. Problem Formulation

The known Shields diagram [2] is the graphical representation of the critical condition for motion initiation. It relates two dimensionless parameters, the Shields parameter Θ and the particle Reynolds Re_p

$$\theta = \frac{\tau_C}{D(\gamma_S - \gamma)} \tag{1}$$

$$\mathrm{Re}_p = \frac{u_* D}{\nu} \tag{2}$$

where τ_c = critical shear stress (N/m^2); D = mean diameter of bed particles (m); γ_s = specific weight of particles (N/m^3); Y = specific weight of the fluid (N/m^3), v = kinematic viscosityof the fluid (m^2/s) and u_* = shear velocity (m/s) ($u_* = (\tau/\rho)^{1/2}$; where ρ = fluid density (kg/m^3)).

Using those parameters and the logarithmic velocity profile, Chien and Wan [1] propose the following equation

$$\frac{U_c}{\sqrt{\frac{\gamma_S - \gamma}{\gamma} gD}} = 5.75\sqrt{f(R_{ep})}\log 12.27\frac{\chi R}{k_S} \tag{3}$$

where U_c = mean critical velocity for motion initiation (m/s), R = hydraulic radius (m), k_s = bed rugosity (m), g = gravity acceleration (m^2/s), X = constant and $f(Rep)$ = function of Re_p or Shields parameter Θ in the bed motion initiation. Considering Shields(1936) results for Re_p larger than 60 the value of Θ is close to 0.045, and equation 3 becomes

$$\frac{U_c}{\sqrt{\frac{\gamma s - \gamma}{\gamma} gD}} = 1.219\log 12.27\frac{\chi R}{k_s} \tag{4}$$

Einstein [20] define X as a function of the relationship k_s/∂, for rough bed $k_s/\partial > 10$, $X = 1$, if $k_s/\partial < 0.25$ then we have smooth bed $X = 0.3u_*k_s/v$; the maximum $X = 1.6$ is obtained in the transition zone for $k_s/\partial = 1.0$; ∂ = is the depth of the viscous sublayer. Some formulas in the scientific literature have the form of equation 4. Between them the equation of Goncharov [21]

$$\frac{U_c}{\sqrt{\frac{\gamma_S - \gamma}{\gamma} gD}} = 1.06\log\frac{8.8h}{D_{95}} \tag{5}$$

where h = flow depth. And the equation of Levy [22]

$$\frac{U_c}{\sqrt{gD}} = 1.4\log\frac{12R}{D_{90}} \tag{6}$$

(2)

The main difference between these formulations is the definition of bed rugosity k_s. For these authors bed rugosity is represented by the largest bed diameter D_{95} or D_{90} respectively ([1] , [6]). Others magnitudes of bed rugosity has been proposed, Ackers and White [1] define $k_s = 1.25\ D_{35}$, Engelund and Hansen [1] propose $k_s = 2\ D_{65}$, Einstein [20] suggest $k_s = D_{65}$. Van Rijn [23] made a review of different authors and conclude that the rugosity of a flat bed and loose varies from 1 to $10D_{90}$ recommending as mean rugosity to be used $k_s = 3\ D_{90}$. It can be said that bed rugosity is defined in the literature as the representative diameter multiplied by a constant larger than one. Engelund and Bayazint (cited by [24]) propose that the representative diameter is the one where settling velocity is equal to the mean settling velocity of the mixture of particles. Logaritmic law of velocity distribution [16] can be expressed as

$$\frac{u}{u_*} = \frac{1}{k}\ln\frac{y}{k_s} + B \tag{7}$$

The constant B included in this logaríthmic velocity distribution has been obtained experimentally using the hydraulic boundary condition. Fuentes and Carrasquel (cited by [16]) propose the following approximation to obtain B as a function of Reynolds of the rugosity R_*.

$$B = -\frac{1}{k}\ln\left[\frac{1}{9.025R_*} + \frac{1}{30}e^{\left(-10.78/R_*\right)}\right] \tag{8}$$

where k = Von Karmar constant, in this case $k = 0.4$ (no suspended solids) [25]. The parameter R_* (Reynolds of the rugosity) is expressed in function of bed rugosity ks

$$R_* = \frac{u_* k_s}{\nu} \tag{9}$$

The Reynolds stress is the term that considers the total shear stress distribution

$$\tau = -\rho\overline{u'v'} = \rho u_*^2\left(1 - {}^{y}/_{h}\right) \tag{10}$$

where y = height above bed; u'= fluctuation velocity in flow direction and v' = vertical fluctuation velocity. This flow distribution has been validated for turbulent open channel flow by [19]. They compare the shear stress based on friction slope S with the one obtained by measuring the Reynolds stress profiles ([26], [27]) . The optical technique PTV used in this work allow us to measure velocity fluctuations and obtain a value of shear velocity u_* ([28], [29]).

2.1 Experimental measurements

Sand from a quartz mine was used to obtain the five (beds) with different D. The density and specific weight are $\rho_s = 2\ 543\ Kg/m^3$ and $\gamma_s = 24\ 950\ N/m^3$. Table 1 presents sand characteristics. An average value D is also presented. The American Geophysical Union classification for each bed is also presented.

Table 1 . Bed characteristics

Loose bed	Maximun Size D_{mx}(mm)	Minimun Size D_{mn}(mm)	Average Size D (mm)	AGU Classification
S1	0.425	0.333	0.379	Medium sand
S2	0.850	0.425	0.638	Coarse sand
S3	1.000	0.850	0.925	Coarse sand
S4	2.360	1.000	1.680	Very coarse sand
S5	4.000	2.360	3.180	Very fine gravel

The experiments for motion initiation were developed in a 120 cm long channel with a width of 10 cm. The sand was colocated in a trench in the middle of the channel with a flat configuration at the start. Figure 1 shows the experimental set up with the accesories used in the optical technique PTV. The analysis region for PTV was the center of the channel parallel to flow direction.

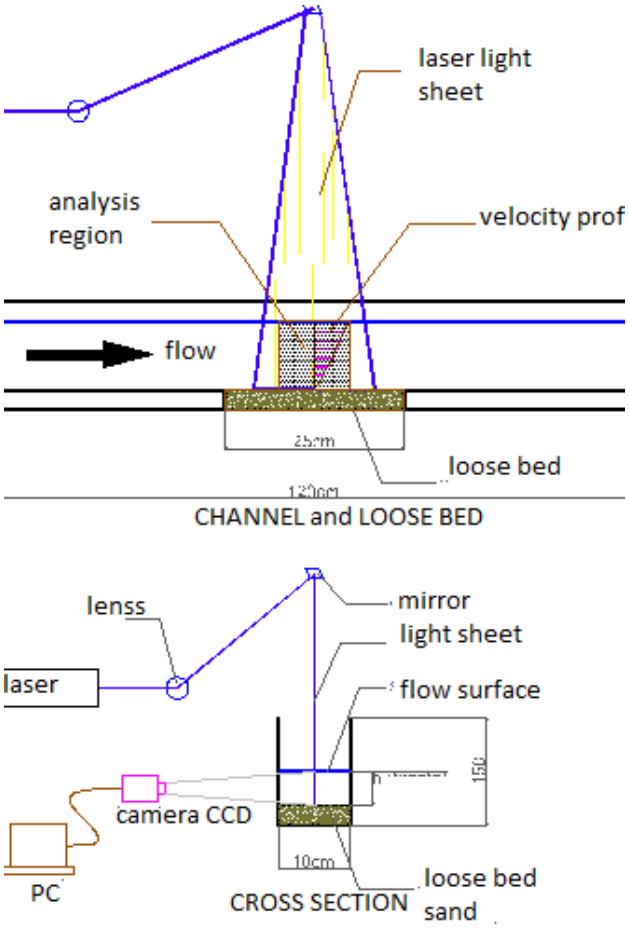

Figure 1 Image capture and processing in a flow region over loose bed

The velocity profiles obtained comes from an average 7000 data of velocity in flow direction, u and the vertical direction, v, at different depths of flow y until h. A cross correlation allowed us to obtain the best fit curve of the form

$$y = Ae^{b_0 u} \tag{11}$$

Where, y = depth over the bed (m), u = velocity in the flow direction (m/s), and A, b_0 regression constants.

Motion initiation was simulated by increasing the flow rate until a visual evident motion of sediment was obtained. Velocity profiles were obtained for flow rates previous to motion initiation and for motion initiation.

Shear velocity was calculated taking into account the Reynolds shear stresses, according to the following equation

$$u_* = (\overline{u'v'})^{1/2} = \sqrt{\frac{1}{N}\sum_{N}^{i=1}(u_i - U_x)(v_i - V_m)} \tag{12}$$

Where U_x = Mean velocity in the flow direction (obtained from experimental data); V_m = mean flow velocity in the vertical direction (obtained from experimental data); *u'* and *v'* are the fluctuating velocities *in x and y* ; and *N* =total velocity data used to perform the regression. The mean velocities U_x and V_m are obtained in the following way

$$U_x = \left[\frac{h}{b_0}\ln\left(\frac{h}{A}\right) - \frac{h}{b_0}\right] + \left[\frac{A}{b_0}\right] \tag{13}$$

$$V_m = \frac{1}{N}\sum_{N}^{i=1} v_i \tag{14}$$

2.2 Bed rugosity determination

From the regression curve of the experimental data and from logarithmic velocity profile equations 15 and 16 are obtained

$$\ln(y) = \ln(A) + b_0 u \tag{15}$$

$$\ln(y) = \frac{k}{u_*}u + \ln(k_s) - Bk \tag{16}$$

Then, the following relationship is obtained from equations 15 and 16

$$\ln(A) = \ln(k_s) - Bk \tag{17}$$

Equation 17 contains two unknowns k_s and the constant *B*. Using an expression for *B* proposed by Fuentes-Carrasquel [16] is written as

$$\ln\left(\frac{k_s}{A}\right) = -\ln\left[\frac{1}{9.025(R_*)} + \frac{1}{30}e^{\left(-10.78/(R_*)\right)}\right] \tag{18}$$

Bed rugosity k_s is obtained by solving equation 18 for the experimental data.

3. RESULTS

Figure 2 shows the data obtained for each sand bed at different runs whit the same rate and the corresponding average velocity profile from correlation analysis.

Simulations of motion initiation were developed for each of the five sand grains. In each simulation an average of 10 velocity profiles were obtained before motion initiation. Figure 3 show results for each sand bed. The maximum velocities applied to the bed *S5 = 3.180mm* were not enough to obtain motion initiation. Table 2 presents mean velocities and shear stresses for the motion initiation of the five beds analized. It includes also the conditions used to start the simulations (minimum flow conditions).

Table 2.- Shear stresses and velocities for motion initiation

Loose bed	Average size *D(mm)*	minimum		motion initiation	
		τ_0 (N/m^2)	U_x (*cm/s*)	τ_c (N/m^2)	U_c (*cm/s*)
S1	0.379	0.196	19.544	0.315	25.809
S2	0.638	0.252	21.764	0.438	27.912
S3	0.925	0.247	23.379	0.554	31.848
S4	1.680	0.412	29.648	0.953	38.202
S5	3.180	0.429	29.315	maximum (no motion)	
				2.253	70.252

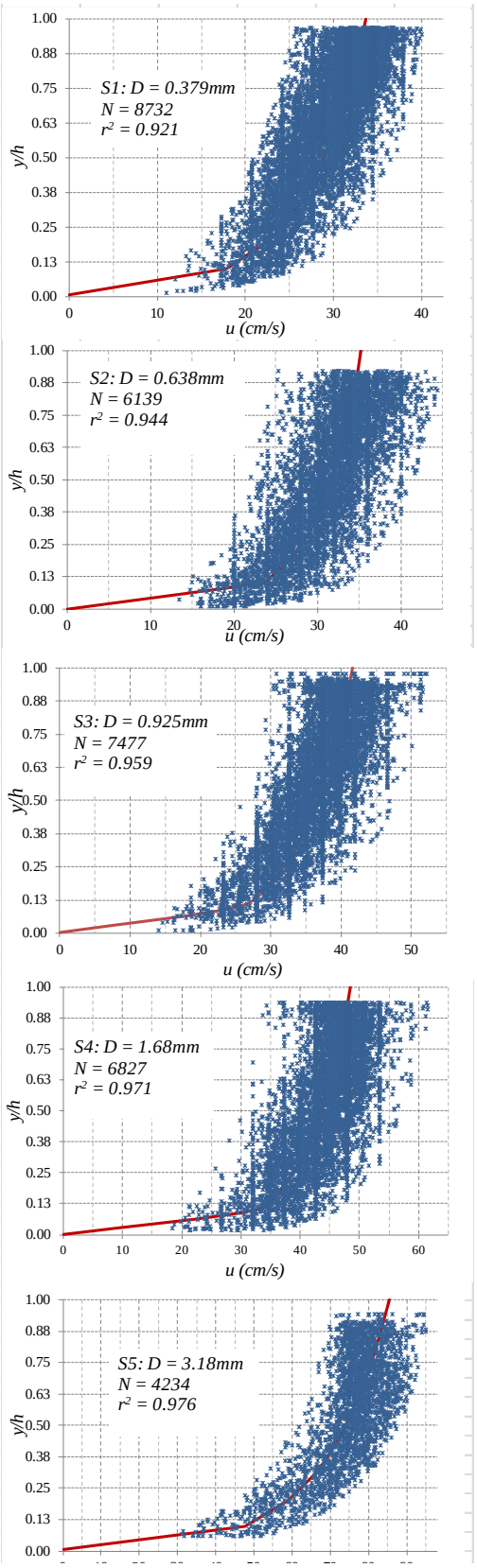

Figure 2. Example of data from PTV and cross-correlation analysis.

Figure 3 shows velocity profiles for each of the sand beds. For the coarse sand bed experimental conditions did not allow us to observe motion initiation thus.

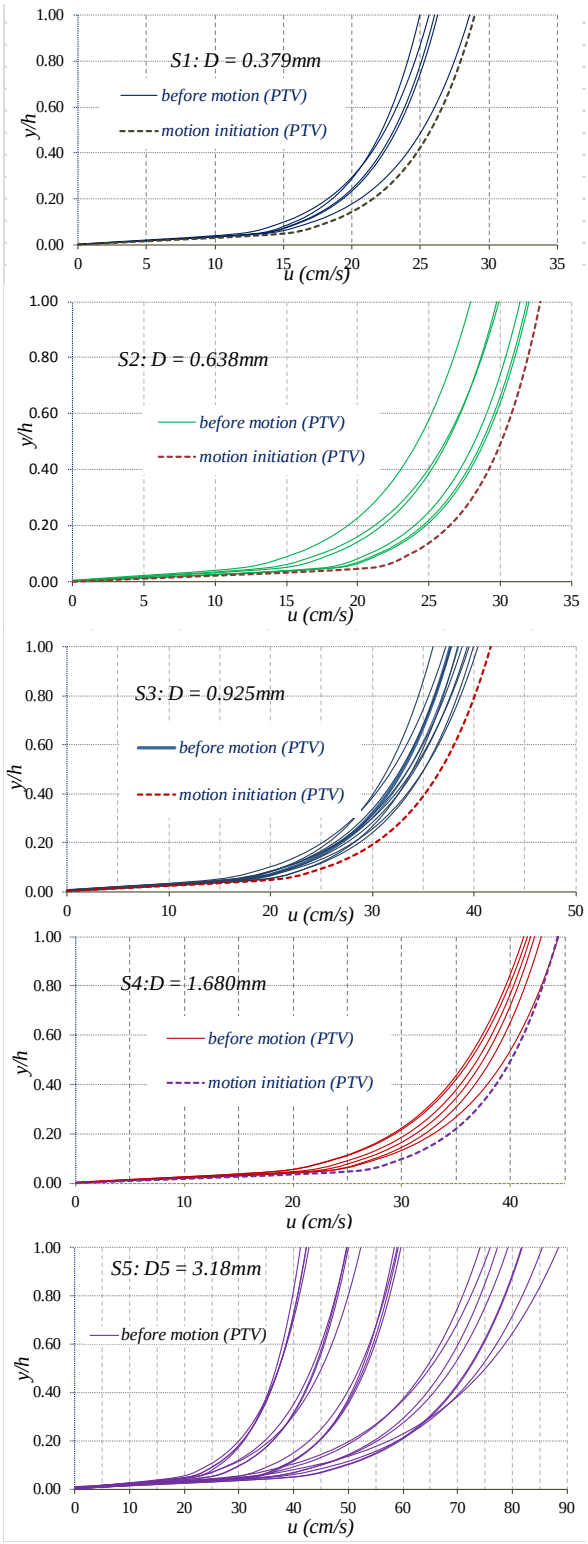

Figure 3. Velocity profiles before motion initiation and for motion initiation

Using equation 18 the values of k_s obtained vary from 5.21 to 0.91 times D for the condition of motion initiation.. The mean rugosity k_s for each bed is

presented in table 3. It is observed that bed rugosity is always larger than D and when D increases, k_s/D decreases.

Table 3.- Experimental bed rugosity k_s and relative rugosity k_s/D.

Loose bed	Average size $D(mm)$	Before and close motion	
		k_s (mm)	k_s/D
S1	0.379	1.733	4.573
S2	0.638	2.029	3.180
S3	0.925	2.909	3.144
S4	1.680	3.775	2.247
S5	3.180	4.847	1.524

Figure 4 shows the relationship between D and the relative rugosity *k*s /D. It can be observed that relative bed rugosity is larger for fine sand than for medium sand and fine gravel.

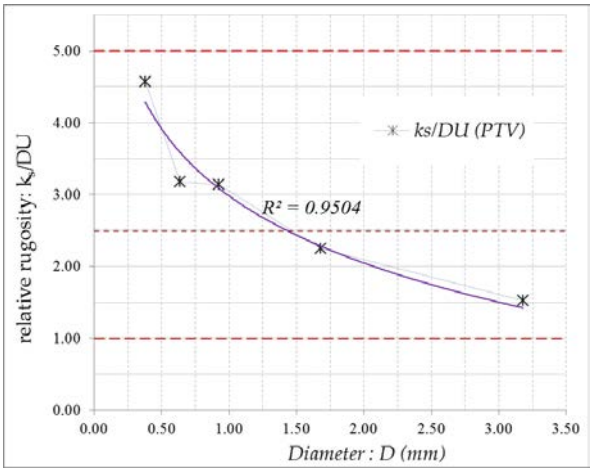

Figure 4-. Relationship between D and k_s/D.

Critical mean velocities are similar to those obtained by Goncharov [21], Levy[22] , Chien and Wan [1] and Fuentes Carrasquel [16]. Table 4 shows this comparison where in the case of Chien and Wan [1], the velocity is defined according to Einstein [20] graph and a bed rugosity $k_s = D_{65}$. In order to use Fuentes Carrasquel expression $k_s = D$ and the experimental critical shear stresses (table 2) . For Goncharov [21] and Levy [22], $k_s = D_{95}$ and $k_s = D_{90}$ respectively. PTV experimental results are also included

Table 4.- Comparison of critical mean velocities

Loose bed	D (mm)	mean	theoretic			
		PTV	Goncharov $k_s = D_{95}$	Levy $k_s = D_{90}$	Chien – Einstein ks = D_{65}	Fuentes - Carrasquel
S1	0.379	25.809	23.929	31.591	28.084	33.581
S2	0.638	27.912	27.365	40.452	32.288	34.970
S3	0.925	31.848	32.899	47.340	36.782	37.428
S4	1.680	38.202	38.356	54.044	42.435	41.791
S5	3.180	no motion 70.252	45.599	64.542	50.325	49.669

As can be seen in table 4 almost all the formulas overestimate the experimental (PTV) mean critical velocity. Only for S5 bed, mean experimental velocity is larger than theoretic. This is the one where no motion initiation was observed, but in this case the shear stress is less than critical theoretic shear stress obtained by de Shields or Yalin-Karahan criteria.

4.- CONCLUSIONS

It has been shown experimentally, that for cohesionless sediments, bed rugosity is larger than mean bed diameter D, which is a common practice in defining bed rugosity. In order to define bed rugosity for sands it should be taken into acount that relative bed rugosity for fine sand is larger than relative rugosity for medium sand and for fine gravel.

In order to apply as criteria for motion initiation the mean critical velocity, it should be used the apropiate bed rugosity that varies with the mean diameter D, according to figure 4. In this figure it is shown, the finding of this research, that relative bed rugosity decreases when the mean diameter D increases.

The experimental critical shear stresses obtained in this work are similar to those obtained by Shields curve.

NOMENCLATURE

B = *constant in logarithmic velocity profile*

b_0, A = *constants in the regression*

D = *Mean particle diameter (mm)*

D_{35} = *Size larger than 35% (mm)*

D_{50} = *Size larger than 50% (mm)*

D_{65} = *Size larger than 65% (mm)*

D_{90} = *Size larger than 90% (mm)*

D_{95} = *Size larger than 95% (mm)*

D_{mn} = *Maximun size of particles(mm)*

D_{mx} = *Minimum size of particles (mm)*

g = *acceleration of gravity*

h = *Flow depth (cm)*

k = *Von Karman constant = 0.4*

k_s = *Bed rugosity (mm)*

R = *Hydraulic radius (mm)*

R_* = *Reynolds of rugosity (-)*

Re_p = *Particle Reynolds (-)*

S = *Friction slope*

S1, S2, S3, S4, S5 = *Different beds*

u = *Mean point velocity (cm/s)*

u_* = *Shear velocity (cm/s)*

u' = *Fluctuating velocity u (cm/s)*

U_c = *Mean critical velocity (cm/s)*

U_x = *Mean flow velocity (cm/s)*

v' = *Fluctuating velocity v (cm/s)*

V_m = *Mean velocity in vertical direction (cm/s)*

y= *Distance from bed (cm)*

□ = *Einstein parameter (-)*

γ_s = *Specific weight of particles (N/m^3)*

v *Kinematic viscosity of water (m/s)*

Θ *Shields parameter (-)*

ρ_s = *Particles density (kg/m^3)*

τ_0 = *Bed shear stress*

τ_c = *Critical shear stress (N/m^2)*

□= *Reynolds stress (N/m^2)*

5. REFERENCES

[1] Chien N. and Wan Z. 1998. *Mechanics of Sediment Transport*; ASCE press, USA.

[2] Shields A. 1936. Anwendung der Aechlichkeitsmechanik und der turbulenzforschung auf die Geschiebewegung. *Mitt. Preussische Versuchsanstalt fur Wasserbau und Schiffbau*. Berlin, Germany.

[3] Yalin M.S. and Arahan E.K. 1979. Inception of sediment transport. *J. Hyd. Div. Proc. Amer. Soc. Civil Engrs*. Vol. 105. No. HY11, pp:1433-1443.

[4] Buffinton John M. 1999. The Legend of A. F. Shields. *Journal of Hydraulic Engineering.* Volume 125, Issue 4, pp. 376-387.

[5] Cao Zhixian; Pender Gareth and Meng Jian; 2006. Explicit Formulation of the Shields Diagram for Incipient motion of sediment. *Journal of Hydraulic Engineering*; Volume 132, Issue 10, pp. 1097-1099.

[7] García Flores Manuel, Maza Álvarez J. A. 1997. *Inicio de Movimiento y Acorazamiento*. Capitulo 8 Manual de Ingeniería de Ríos,UNAM-México.

[8] Ling Chi-Hai; 1995. Criteria for Incipient Motion of Spherical Sediment Particles. *Journal of Hydraulic Engineering*. Volume 121, Issue 6, pp. 472-478.

[9] Smith David A. 2004. Initiation of Motion of Calcareous Sand. *Journal of Hydraulic Engineering*. Volume 130, Issue 5, pp. 467-472

[10] Dancey Clinton L. Diplas P. Papanicolaou A. Bala Mahesh. 2002. Probability of individual grain movement and threshold condition. *Journal of Hydraulic Engineering*. Volume 128, Issue 12, pp. 1069-1075.

[11] Garde R. J; Sahay A. and Bhatnagar S. 2006. A simple mathematical model to predict the particle size distribution of the armour layer. *Journal of Hydraulic Engineering and Research*. Volume 38, Issue 5, pp. 815-821.

[12] Papanicolaou A.N. 2002. Stochastic Incipient Motion Criterion for Spheres under Various Bed Packing Conditions. *Journal of Hydraulic Engineering*; Volume 128, Issue 4, pp. 369-380.

[13] Hunziker Roni P. and Jaeggi Martin N. R. 2002. Grain sorting processes. *Journal of Hydraulic Engineering*. Volume 128, Issue 12, pp. 1060-1068.

[14] Kuhnle Roger A. 1993. Incipient Motion of Sand-Gravel Sediment Mixtures. *Journal of Hydraulic Engineering*. Volume 119, Issue 12, pp. 1401-1414.

[15] Sarmiento O. A. and Falcon M. A. 2006. Critical bed Shear Stress for unisize sediment. *Journal of Hydraulic Engineering.* Volume 132, Issue 2, pp. 172-179.

[16] Maza Álvarez J. A. García Flores M. 1984. *Hidrodinámica Bases para hidráulica fluvial*. Ed. Instituto de Ingeniería, UNAM-México.

[17] Salinas Tapia H. 2007. *Determinación de parámetros para flujo bifásico, sólido-líquido, aplicando técnicas ópticas.* Doctoral thesis. CIRA-Fac. Eng.-Universidad Autónoma del Estado de Mexico-México.

[18] Yang Shu-Qing, and McCorquodale John A. 2004; Determination of Boundary Shear and Reynolds Shear in Smooth Rectangular Channel Flows. *Journal of Hydraulic Engineering.* Volume 130, Issue 5, pp. 458-462.

[19] Lemmin Ulrich and Rolland Thierry. 1997. Acoustic Velocity Profiler for Laboratory and field Studies. *Journal of Hydraulic Engineering.* Volume 123, Issue 12, pp. 1089-1098.

[20] Einstein H.A. 1950. The bed load function of sediment transportation in open channel flows. US. Dept. Agri., technical bulletin 1026.

[21] Goncharov V.N. 1962. Basic river dynamics. *Hydro-Meteorological press*, Leningrad, Russia.

[22] Levy E.E. 1956. River Mechanics, *National Energy Press*, Moscow, Russia..

[23] Van Rijn L. 1982. Equivalent roughness of alluvial bed. *Journal of Hydraulic Engineering.* Volume 108, Issue 10, pp. 1215-1218.

[24] Smart Graeme M. 1999. Turbulent Velocity Profiles and Boundary Shear in Gravel bed Rivers. *Journal of Hydraulic Engineering*. Volume 125, Issue 3, pp. 106-116.

[25] Cheng Nian-Sheng and Chiew Yee-Meng**.** 1998. Modified logarithmic law for velocity distribution subjected to upward seepage. *Journal of Hydraulic Engineering*. Volume 124, Issue 12, pp. 1235-1241.

[26] Best Jim, Bennet Sean, Brige John and Leeder Mike. 1997. Turbulence modulation and particle velocities over flat sand beds at low transport rates. *Journal of Hydraulic Engineering*. Volume 123, Issue 12, pp. 1118-1130.

[27] Song T. and Graf W. H. 1996. Velocity and Turbulence Distribution in Unsteady Open Channel Flows. *Journal of Hydraulic Engineering.* Volume 122, Issue 3, pp. 141-196.

[28] Adrian Ronald J. 1991. Particle-Imaging techniques for experimental fluid mechanics. *Annual Review of Fluid Mechanics*. Volume 123; p.p. 43-6.

[29] Salinas Tapia H, García Aragón J.A., Moreno D. y Barrientos B., 2006. *Particle Tracking Velocimetry (PTV) Algorithm for non-uniform and non-spherical Particles. Proceedings Electronics, Robotics and Automotive Mechanics Conference, CERMA 06-IEEE computer society. , Vol II. Cuernavaca-México.*